

Next Generation Very Large Array Memo #55 Taperability Study for the ngVLA and Performance Estimates (v2)

Viviana Rosero (NRAO)

December 9, 2019

Abstract

In this memo I use taperability as a metric to compare six different subarrays that are part of the current ngVLA reference design (Rev. C) using simulations at 30 GHz. These subarrays consist of antennas selected from the Main array and the Long Baseline Array, up to a total of 244 18 m antennas; the short baseline array is also part of the reference design but is not considered in this work. I present a study of the simulated image noise at different angular resolutions, achieved by varying the imaging weights, and I show examples of how combinations of robustness and tapering allow for a beam of much higher quality at the expense of sensitivity. For each of these six subarrays, I use the resulting taperabilities to estimate the sensitivities and key performance metrics over a range of resolutions.

1 Introduction

The ngVLA is designed to accommodate a wide variety of scientific observations with a non-reconfigurable array, which means it needs to deliver high sensitivity over a range of resolutions. There are five key science goals (KSG) whose requirements are the main drivers of the array design:

- **KSG 1:** Unveiling the Formation of Solar System Analogs on Terrestrial Scales
- **KSG 2:** Probing the Initial Conditions for Planetary Systems and Life with Astrochemistry
- **KSG 3:** Charting the Assembly, Structure, and Evolution of Galaxies from the First Billion Years to the Present
- **KSG 4:** Using Pulsars in the Galactic Center to Make a Fundamental Test of Gravity

- **KSG 5:** Understanding the Formation and Evolution of Stellar and Supermassive Black Holes in the Era of Multi-Messenger Astronomy

For more on the specific requirements of the KSGs see ngVLA Science Requirements document [8] and ngVLA memo #19 [1]. Several memos have explored the array performance of different key science goals, for instance KSG 3 and KSG 1 have been analyzed in ngVLA memo #13 [3] and ngVLA memo #33 [9], respectively.

The present reference ngVLA array design (October 2018) includes three fundamental subarrays:

- A Main Interferometric Array (also known as the Spiral214) of 214 x 18 m antennas
- A Short Baseline Array (SBA) of 19 x 6 m antennas
- A Long Baseline Array (LBA) of 30 x 18 m antennas

Antennas within the Main array are distributed over a range of physical scales and with different geometries: i) a dense Core which provides high surface brightness sensitivity at $\sim 1,000$ mas resolution (at 30 GHz) needed for KSG 3; b) a multi-arm spiral – located within the Plains of San Agustin, NM – capable of high-fidelity imaging at ~ 100 mas scales important for KSGs 2 and 3; c) longer arms which provide mid-scale baselines for imaging at ~ 10 mas required for KSGs 1 and 2. The Main array will be augmented by a very compact array of smaller antennas (SBA) which will provide sensitivity on larger angular scales, and four antennas of the Main array will be equipped to measure total power in order to fill in the center of the (u,v)-plane. Additionally, a Long Baseline Array (LBA) consisting of several outlying stations will provide intercontinental-scale baselines for achieving resolutions of ~ 0.1 mas needed for KSGs 4 and 5. In this memo I will analyze the reference design, composed of the Main and Long Baseline Array for a total of 244 18 m antennas, and selected subarrays within the reference design; the SBA will be addressed in a future work.

In ngVLA memo #3 [7], B. Clark introduced the term *taperability* as a metric to compare arrays, and to understand how well the array can perform at both high and low resolutions as measured in terms of relative sensitivity. Following that concept, in this memo I use taperability as a metric to compare different subarrays from the current design of the ngVLA. Specifically, I will discuss the six subarrays listed in Table 1.

As it has been discussed in previous memos by C. Carilli (e.g., ngVLA memo #12 [2] and ngVLA memo #41 [5]) the centrally condensed antenna distribution of the ngVLA leads to a naturally weighted beam that is not well characterized by a Gaussian function. Specifically, the long baselines produce a very narrow peak in the point spread function (PSF) and the Core contributes a broad

Table 1: Simulations for different subarrays.

Subarray	min. baseline [km]	max. baseline [km]	# antennas
Main+LBA	0.027	8856.4	244
LBA	32.6 ^a	8856.4	30
Main	0.027	1005.4	214
Mid-baseline ^b	7.747	1005.4	46
Plains + Core	0.027	36.5	168
Core	0.027	1.3	94

^aExcluding the very short baselines within stations

^bMain - (Plains+Core)

Note: Columns 2 and 3 are the *projected* baseline lengths for the 4-hour simulations presented in this work and are measured with the CASA function `ms.range`.

skirt (as seen in Figure 1). Specific science applications may need to adjust the uv-weighting and other image parameters to ‘sculpt’ a synthesized beam that is suitable for the particular science goal being considered (ngVLA memo #47 [6]). One of the classic PSF metrics is the height of the first sidelobe, however as we see in Figure 1, the ngVLA’s natural PSF is lacking an obvious first sidelobe and so new beam quality metrics are required. The exploration of such metrics will be presented in a coming memo.

In this memo I expand on some of the work that C. Carilli presented in ngVLA memos #16 [4] and #47 [6] using the current reference design of the ngVLA Rev. C (Main+LBA). I analyze the taperability for each of the subarrays listed in Table 1, and I present results that allow for the incorporation of imaging weights into the sensitivity calculations.

2 Description of the Simulations and Imaging

The simulations presented in this memo were performed using the simulator tool in CASA, and are for a field at +24° Declination observed for 4 hours centered on transit. These simulations do not contain any sources in the field since in this memo I am only interested in the resulting PSFs and an analysis of the image noise. The simulations have a center frequency of 30 GHz and are composed of 1 channel with a frequency resolution of 1 MHz, bandwidth of 1 MHz and integration time of 1s^a. The numbers of antennas used for each of the subarrays

^aAn integration time of 1s is not within the time-smearing limits for some of the considered subarrays, but was chosen to make the simulations faster. Future simulations may need to

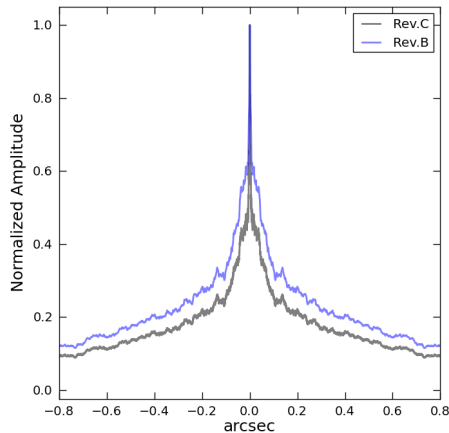


Figure 1: Natural PSF of Rev. B vs Rev. C at 30 GHz.

are listed in Table 1.

The imaging was done using CASA task `tclean`. For each subarray I used the following scheme to determine the imaging parameters:

- *Robust*: I used three categories: (i) Briggs weighting, changing the robust value from uniform ($R = -2$) to close to $R = +1$ and without a uv-taper, allowing for the highest resolutions; (ii) Natural weighting and only changing the uv-taper, to achieve a range of lower resolutions ; (iii) Briggs weighting with a robust value $R = -0.5$ and changing the uv-taper, which is an attempt to sculpt the beam over a range of lower resolutions in a way that greatly reduces the skirt without too much loss in sensitivity.
- *Taper*: I selected the uv-taper based on the minimum and maximum baselines present in the subarray in order to properly obtain the expected resolutions.
- *Cell size*: I chose cell sizes that provide at least four pixels across the PSF full width at half maximum (FWHM), ensure that the resolution could be adequately measured and that all data was gridded.
- *Image size*: The images are large enough (when possible, see §3.1) to adequately measure the noise and capture the broad skirt of the PSF.

The specific parameters used during imaging are presented in §3. A sample of the script used to make the simulations is shown in Appendix B.

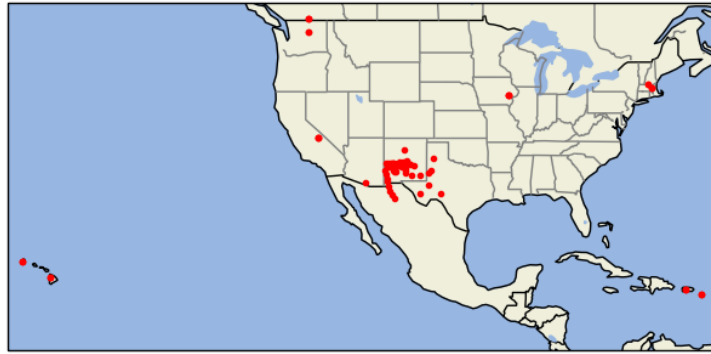
reconsider this value.

3 Sensitivity vs Resolution for different Subarrays

Tables 2, 3, 4, 5, 6 and 7 in Appendix C show the simulation parameters for each of the subarrays studied in this memo. Columns 1, 2 and 3 are the robust, uv-taper and cell size values, respectively. Column 4 gives the full width at half maximum (FWHM) of the major and minor axes of the synthesized beam, as parameterized by Gaussian fitting in the CASA `tclean` task. For the statistics, I report in Columns 5 and 6 the RMS and the standard deviation (σ), respectively, scaled relative to that of the naturally weighted image (i.e., $\text{rms}/\text{rms}_{NA}$ and σ/σ_{NA}). The standard deviation σ takes into account any zero-level offsets and typically provides a better estimate of the image sensitivity when the image mean is non-zero.

Figures 3, 6, 9, 12, 15 and 18 show the change in sensitivity with resolution, i.e., the taperability, at 30 GHz for each simulations. The plotted resolutions ($\theta_{1/2}$) correspond to the geometric mean of the minor and major beam FWHM reported in the tables of simulation parameters. In order to account for the change in sensitivity due to use of imaging weights (relative to the naturally weighted rms defined as σ_{NA}), we have adopted an efficiency factor η_{weight} such that the expected image rms after weighting is $\eta_{weight} \sigma_{NA}$. The sensitivity calculations in the key performance tables include η_{weight} , estimated using the blue and red data series in the taperability figures and by scaling $\theta_{1/2}$ with frequency ($\theta_{1/2} \times \nu/30$ GHz; see Appendix A).

3.1 ngVLA: Main+LBA



Antenna Positions for ngVLA

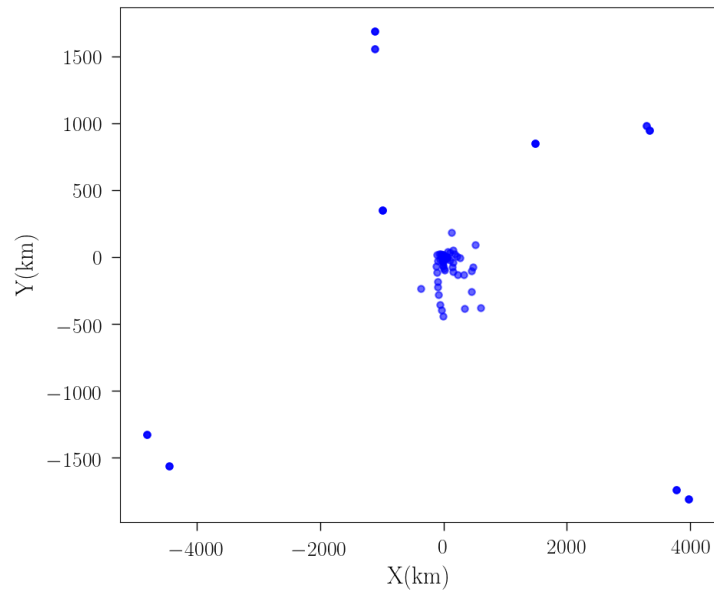


Figure 2: Positions of the 244 18 m antennas for the Main+LBA array.

Figure 2 shows the position of the antennas in the Main+LBA configuration, which spans a maximum baseline of 8856.4 km. For this subarray, all the simulated images with robust $R = -0.5$ have an image size of 35000 pixels and all other images have a size of 10240 pixels. As we can see in Table 2, the measured image RMS does not appear to be consistent with the standard deviation σ due to a non-zero image mean, and for this reason I use values of σ in the analysis of this subarray. For all of the other subarrays studied in this memo, I use

the RMS values since the image mean was approximately zero. Note that the images of the Main+LBA subarray have a small field of view compared to the angular scales of the shortest baselines (which is likely related to the non-zero image mean) but it would be impractical to make the images much larger due to CASA’s memory usage. This raises some concerns about how CASA is gridding the shortest baselines for this subarray, e.g., as part of the zero-spacing flux, but this is beyond the scope of this memo.

Natural weighting with no uv-taper, which gives the best sensitivity, produces an angular resolution of 0.96 mas. From Figure 3 we see that for natural weighting, we can use a uv-taper to vary the angular resolution over a range of $\theta_{1/2} \sim 0.47 - 1163$ mas for which we pay less than a factor of two in sensitivity. Likewise, for the range of angular resolution of $\theta_{1/2} \sim 0.539 - 239$ mas we pay a penalty in sensitivity of $\lesssim 1.5$.

It is interesting to notice some features in the resulting taperability curve, for instance when using natural weighting with uv-taper it appears that the variation in sensitivity is small and smooth over a range of angular resolutions of $\sim 3 - 300$ mas. This makes sense since the LBA provides far fewer baselines than the inner subarrays, thus when using small uv-tapers we are only down-weighting a few of the outermost antennas. Additionally, when using robust values close to uniform without uv-taper the loss in sensitivity is very high and steep since we are suppressing a large number of the shortest baselines (which make up the majority of the total baselines).

Figure 4 shows examples of 1D East-West cuts through example PSFs. In general, as already shown by C. Carilli in ngVLA memo #47 [6] we see that for the naturally weighted beams (both tapered and untapered) the skirt of the PSF is very broad. It was suggested in memo #47 that a skirt at a level of 10% at a radius of one FWHM may be acceptably low (for comparison, a Gaussian beam is $\sim 6\%$ at a radius of one FWHM). At this radius, the naturally weighted beams in Figure 4 are far above 10%, but drop to below or about 10% when a robust value of $R = -0.5$ is used. However, the image noise increases by an additional factor of ~ 1.5 over the increase resulting from using a uv-taper alone.

Table 8 in Appendix D shows the key performance metrics of the ngVLA array using 244 antennas, tabulated for a range of selected resolutions between 0.1 and 1000 mas. These metrics include the change in sensitivity corresponding to the uv-taper needed to achieve these resolutions (based on Figure 3 and the frequency scaling described in Section 3).

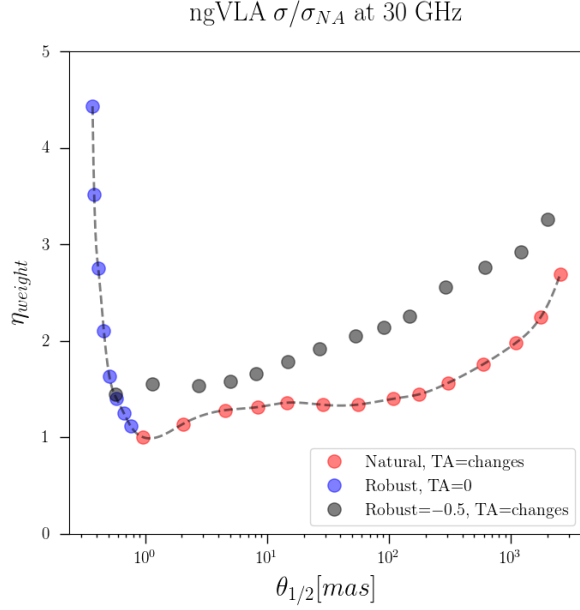


Figure 3: Taperability curve for the present ngVLA reference design showing the image standard deviation (σ) at different angular resolutions (FWHM) achieved by varying the imaging weights, simulated at 30 GHz. The noise has been scaled relative to that of the naturally weighted image (σ_{NA}). The red symbols correspond to use of a uv-taper and natural weights, and the blue symbols to Briggs robust weighting without a taper. The gray symbols are for Briggs robust $R = -0.5$ and a varying uv-taper, which has a large effect on beam quality (see Figure 4). The dashed line is the interpolation of the points used to estimate η_{weight} .

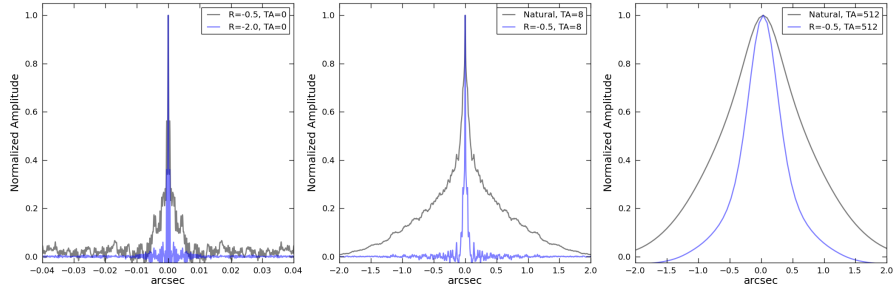


Figure 4: Simulated 30 GHz PSFs for the present ngVLA reference design over a range of resolutions, showing the effect of different imaging weights (TA: uv-taper in mas, R: Briggs robust parameter). The PSFs are a selection of the data presented in Table 2. These examples illustrate how combinations of robustness and tapering allow for a beam of much higher quality (but at the expense of sensitivity).

3.2 ngVLA LBA subarray

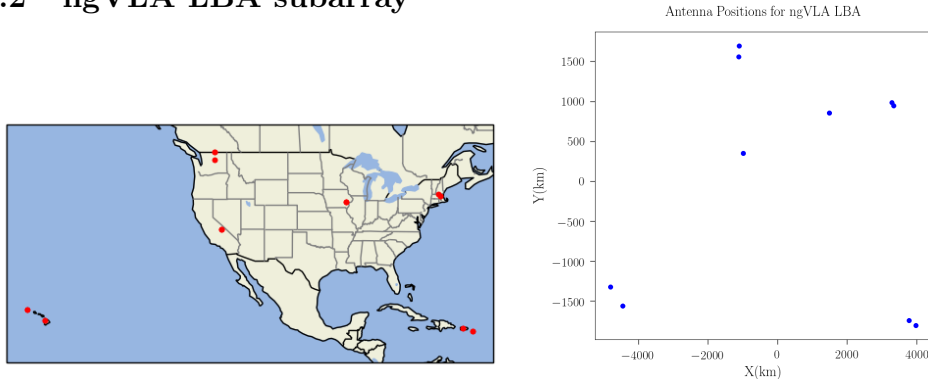


Figure 5: Positions of the 10 stations, composed of 30 18 m antennas, for the LBA subarray.

Figure 5 shows the position of the antennas of the LBA subarray, which extends over a maximum baseline of 8856.4 km. For this subarray, the simulated images have a size of 40000 px and we have excluded the very short baselines within stations by setting $uv_{min} = 32$ km. A uv-range was used here to avoid the issue with a non-zero image mean encountered with the Main+LBA simulations.

Natural weighting with no uv-taper, which gives the best sensitivity, produces an angular resolution of 0.29 mas. From Figure 6 we see that for natural weighting, we can use a uv-taper to vary the angular resolution over a range of $\theta_{1/2} \sim 0.23 - 0.80$ mas for which we pay a penalty in sensitivity of $\lesssim 2$. Likewise, for a range of angular resolution of $\theta_{1/2} \sim 0.235 - 0.55$ mas we pay a penalty in sensitivity of $\lesssim 1.5$.

Figure 7 shows examples of 1D East-West cuts through example PSFs. It is important to point out that the grating response (i.e., the high, persistent sidelobes) is a direct consequence of the uv-coverage of this simulation. For example, a 1D North-South cut does not show the high level of ringing seen in Figure 7. The grating response could be mitigated by using wide-band synthesis, improved earth rotation synthesis, or a distribution of antennas having additional North-South baselines. Notice that for the PSFs without uv-taper (left panel) all values of robust (including natural) appear very similar. When using a modest UV-taper, a robust value of $R = -0.5$ appears to help lowering the sidelobes but at the expense of an additional noise increase. However, when the UV-taper becomes larger (e.g., 2 mas) the sidelobe levels increase, presumably due to downweighting the majority of data.

Table 9 in Appendix D shows the key performance metrics of the ngVLA LBA subarray using 30 antennas, tabulated for a range of selected resolutions between 0.1 and 10 mas. These metrics include the change in sensitivity corresponding to the uv-taper needed to achieve these resolutions (based on Figure 6 and the frequency scaling described in Section 3).

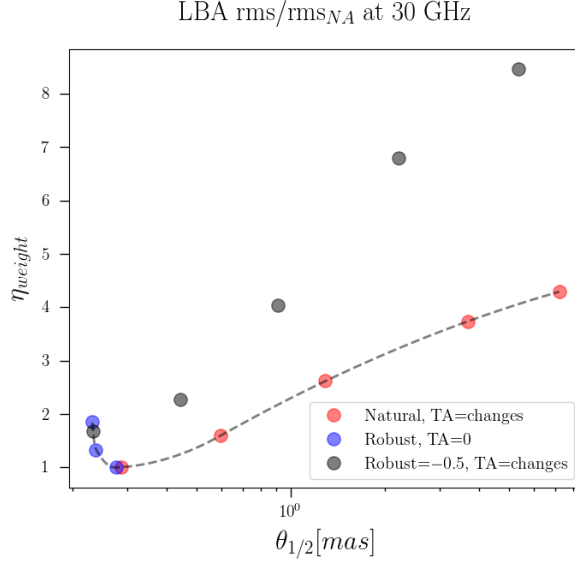


Figure 6: Taperability curve for the ngVLA LBA subarray showing the image noise (rms) at different angular resolutions (FWHM) achieved by varying the imaging weights, simulated at 30 GHz. The noise has been scaled relative to that of the naturally weighted image (rms_{NA}). Symbols and colors are the same as used in Figure 3.

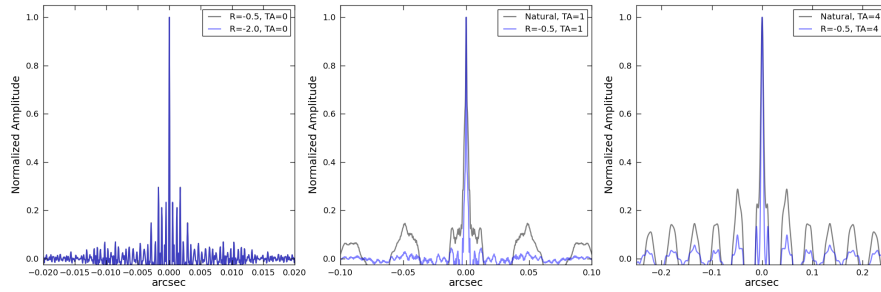


Figure 7: Simulated 30 GHz PSFs for the ngVLA LBA subarray over a range of resolutions, showing the effect of different imaging weights (TA: uv-taper in mas, R: Briggs robust parameter). The PSFs are a selection of the data presented in Table 3. These examples illustrate how combinations of robustness and tapering allow for a beam of much higher quality (but at the expense of sensitivity).

3.3 ngVLA Main subarray

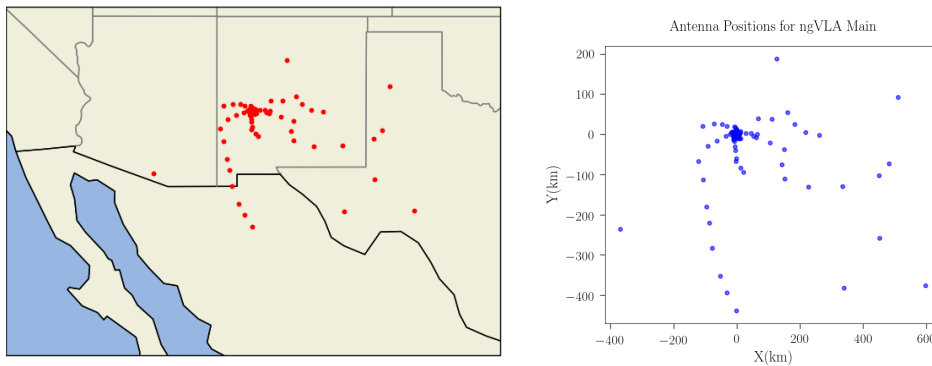


Figure 8: Positions of the 214 18 m antennas for the Main subarray.

Figure 8 shows the position of the antennas of the Main subarray, which extends over a maximum baseline of 1005.4 km. For this subarray, the simulated images have a size of 40000 px. Natural weighting with no uv-taper, which gives the best sensitivity, produces an angular resolution of 8.46 mas. From Figure 9 we see that for natural weighting, we can use a uv-taper to vary the angular resolution over a range of $\theta_{1/2} \sim 3.462 - 1039$ mas for which we pay a penalty in sensitivity of $\lesssim 2$. Likewise, for a range of angular resolution of $\theta_{1/2} \sim 4.212 - 289$ mas we pay a penalty in sensitivity of $\lesssim 1.5$.

Similar to the ngVLA reference configuration (Main+LBA), the resulting taperability curve from natural weighting with uv-taper is relatively shallow over a range of angular resolutions of $\sim 10 - 200$ mas. This is again a consequence of having more short baselines than long, so as we use uv-tapers $\gtrsim 200$ mas the loss in sensitivity increases rapidly since we are downweighting a lot of baselines in the core.

Figure 10 shows examples of 1D East-West cuts through example PSFs. The results are similar to those found with the Main+LBA configuration where at a radius of one FWHM the naturally weighted beam are above 10% but the skirt drops to below or about 10% when using a robust value of $R = -0.5$ at the expense of an additional noise increase than from only using a uv-taper.

Table 10 in Appendix D shows the key performance metrics of the ngVLA Main subarray using 214 antennas, tabulated for a range of selected resolutions between 10 and 1000 mas. These metrics include the change in sensitivity corresponding to the uv-taper needed to achieve these resolutions (based on Figure 9 and the frequency scaling described in Section 3).

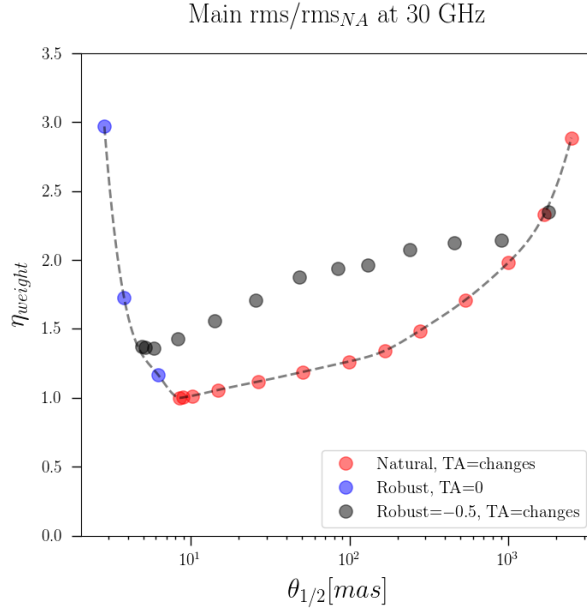


Figure 9: Taperability curve for the ngVLA Main subarray showing the image noise (rms) at different angular resolutions (FWHM) achieved by varying the imaging weights, simulated at 30 GHz. The noise has been scaled relative to that of the naturally weighted image (rms_{NA}). Symbols and colors are the same as used in Figure 3.

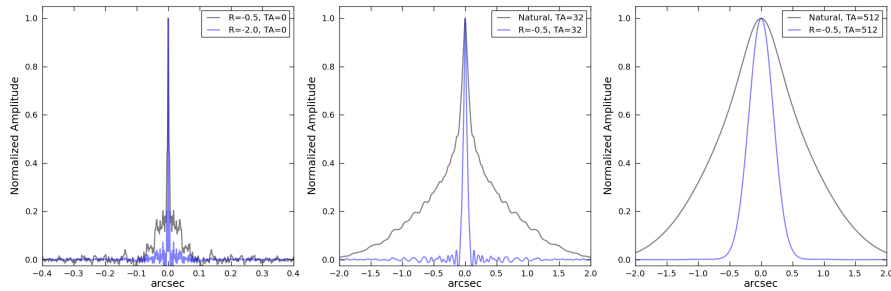


Figure 10: Simulated 30 GHz PSFs for the ngVLA Main subarray over a range of resolutions, showing the effect of different imaging weights (TA: uv-taper in mas, R: Briggs robust parameter). The PSFs are a selection of the data presented in Table 4. These examples illustrate how combinations of robustness and tapering allow for a beam of much higher quality (but at the expense of sensitivity).

3.4 ngVLA Mid-baseline subarray

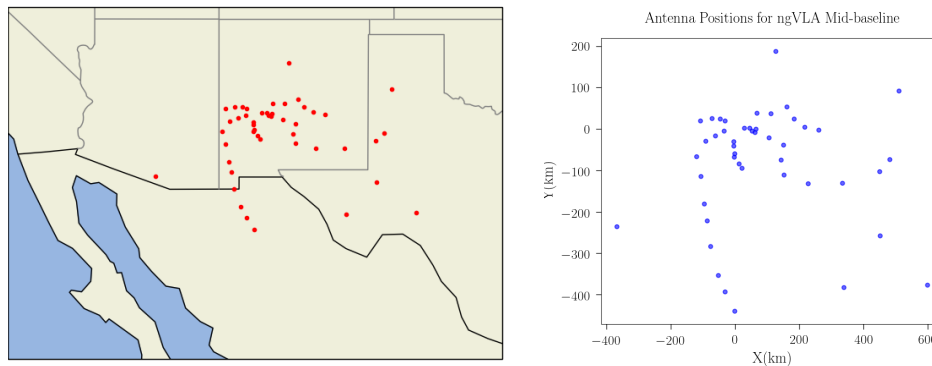


Figure 11: Positions of the 46 18 m antennas for the Mid-baseline subarray.

Figure 11 shows the position of the antennas of the Mid-baseline subarray, which consists of all antennas that are not in the LBA, Plains or Core subarrays and extends over a maximum baseline of 1005.4 km. For this subarray, the images have a size of 40000 px.

Natural weighting with no uv-taper, which gives the best sensitivity, produces an angular resolution of 3.49 mas. From Figure 12 we see that for natural weighting, we can use a uv-taper to vary the angular resolution over a range of $\theta_{1/2} \sim 2.4 - 13$ mas for which we pay a penalty in sensitivity of $\lesssim 2$. Likewise, for a range of angular resolution of $\theta_{1/2} \sim 2.5 - 8.7$ mas we pay a penalty in sensitivity of $\lesssim 1.5$.

Without the short baselines provided by the antennas in the Plains and the Core the loss of sensitivity as we use larger uv-tapers is more steep.

Figure 13 shows examples of 1D East-West cuts through example PSFs. This specific configuration does not have the dense Core and, thus the PSF profiles do not have the undesired broad skirt. We can see that natural weighting with uv-taper produces a very similar PSF than using robust $R = -0.5$ but without losing the additional sensitivity.

Table 11 in Appendix D shows the key performance metrics of the ngVLA Mid-baseline subarray using 46 antennas, tabulated for a range of selected resolutions between 1 and 100 mas. These metrics include the change in sensitivity corresponding to the uv-taper needed to achieve these resolutions (based on Figure 12 and the frequency scaling described in Section 3).

Mid-baseline rms/rms_{NA} at 30 GHz

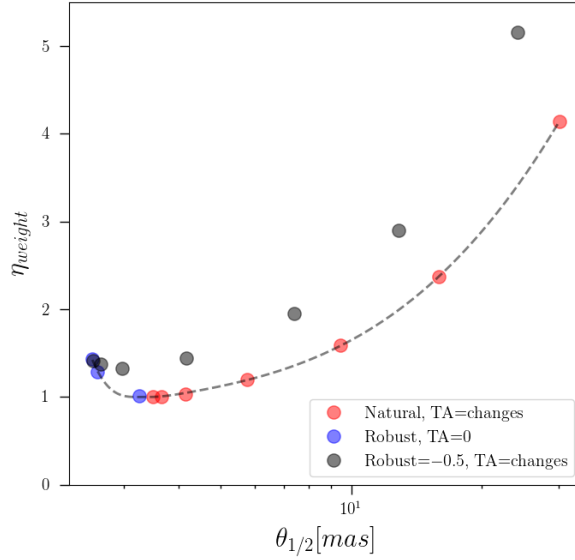


Figure 12: Taperability curve for the ngVLA Mid-baseline subarray showing the image noise (rms) at different angular resolutions (FWHM) achieved by varying the imaging weights, simulated at 30 GHz. The noise has been scaled relative to that of the naturally weighted image (rms_{NA}). Symbols and colors are the same as used in Figure 3.

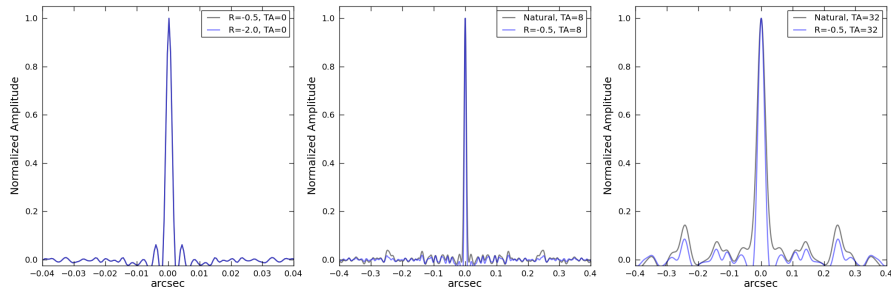


Figure 13: Simulated 30 GHz PSFs for the ngVLA Mid-baseline subarray over a range of resolutions, showing the effect of different imaging weights (TA: uv-taper in mas, R: Briggs robust parameter). The PSFs are a selection of the data presented in Table 5. These examples illustrate how combinations of robustness and tapering allow for a beam of much higher quality (but at the expense of sensitivity).

3.5 ngVLA Plains+Core Subarray

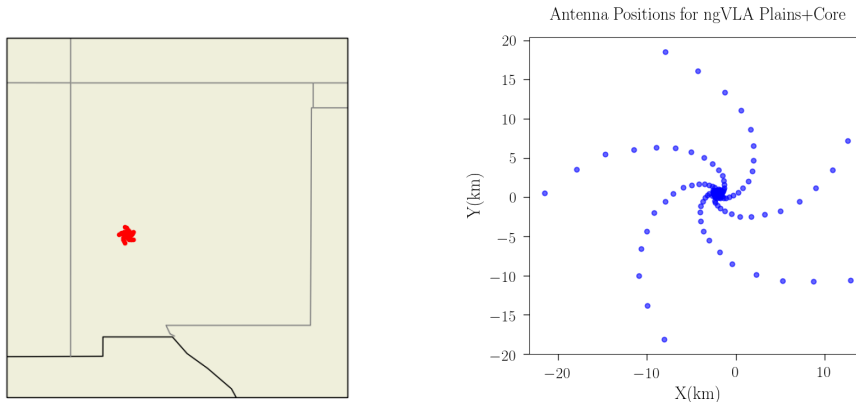


Figure 14: Positions of the 168 18 m antennas for the Plains+Core subarray.

Figure 14 shows the position of the antennas of the Plains+Core subarray, which extends over a maximum baseline of 36.5 km. For this subarray, the images have a size of 20480 px.

Natural weighting with no uv-taper, which gives the best sensitivity, produces an angular resolution of 163.05 mas. From Figure 15 we see that for natural weighting, we can use a uv-taper to vary the angular resolution over a range of $\theta_{1/2} \sim 76.71 - 2710$ mas for which we pay a penalty in sensitivity of $\lesssim 2$. Likewise, for a range of angular resolution of $\theta_{1/2} \sim 86.97 - 1324$ mas we pay a penalty in sensitivity of $\lesssim 1.5$.

The features of the resulting taperability curve are similar to the ones from the ngVLA Main subarray, likely due to their similar ratios of short versus long baselines (i.e., many more short baselines than long baselines).

Figure 16 shows examples of 1D East-West cuts through example PSFs. At the lower resolutions the beams have a broad skirt when using natural weighting, as was the case for the Main and Main+LBA subarrays.

Table 12 in Appendix D shows the key performance metrics of the ngVLA Plains+Core subarray using 168 antennas, tabulated for a range of selected resolutions between 100 and 10000 mas. These metrics include the change in sensitivity corresponding to the uv-taper needed to achieve these resolutions (based on Figure 15 and the frequency scaling described in Section 3).

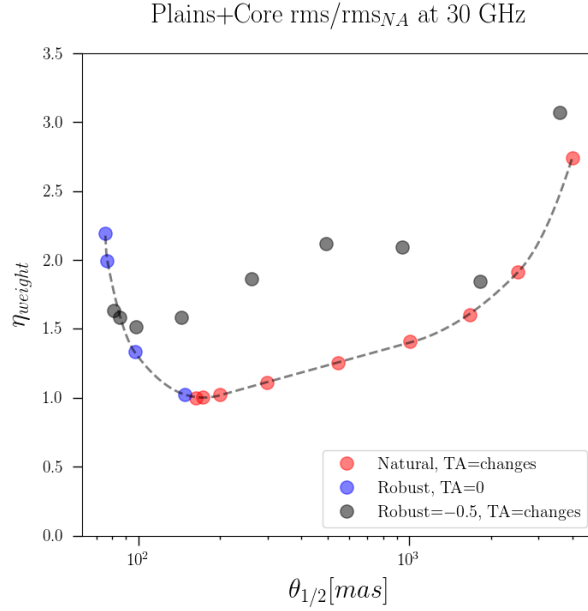


Figure 15: Taperability curve for the ngVLA Plains+Core subarray showing the image noise (rms) at different angular resolutions (FWHM) achieved by varying the imaging weights, simulated at 30 GHz. The noise has been scaled relative to that of the naturally weighted image (rms_{NA}). Symbols and colors are the same as used in Figure 3.

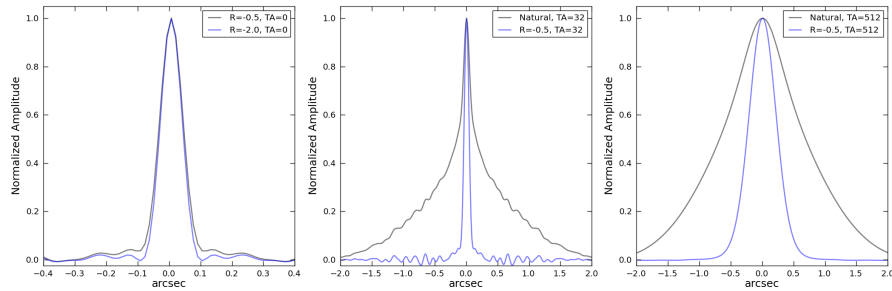


Figure 16: Simulated 30 GHz PSFs for the ngVLA Plains+Core subarray over a range of resolutions, showing the effect of different imaging weights (TA: uv-taper in mas, R: Briggs robust parameter). The PSFs are a selection of the data presented in Table 6. These examples illustrate how combinations of robustness and tapering allow for a beam of much higher quality (but at the expense of sensitivity).

3.6 ngVLA Core Subarray

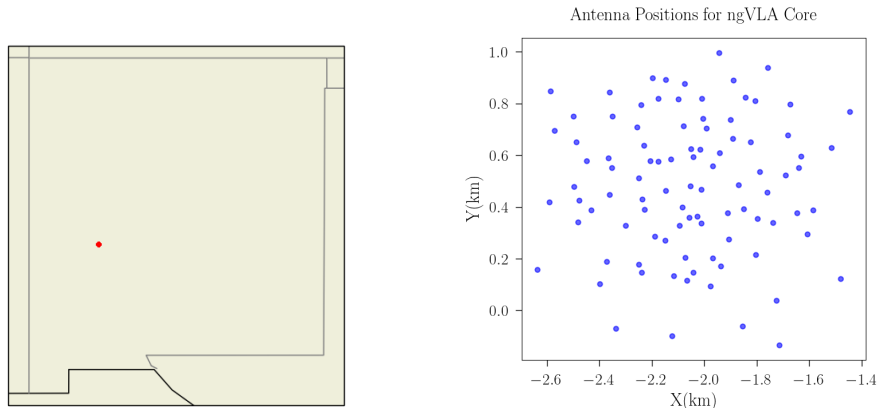


Figure 17: Positions of the 94 18m antennas for the Core subarray.

Figure 17 shows the position of the antennas in the Core subarray, which extends over a maximum baseline of 1.3 km. For this subarray, the simulated images have a size of 10240 px.

Natural weighting with no uv-taper, which gives the best sensitivity, produces an angular resolution of 2041 mas. From Figure 18 we see that for natural weighting, we can use a uv-taper to vary the angular resolution over a range of $\theta_{1/2} \sim 1580 - 5150$ mas for which we pay a penalty in sensitivity of $\lesssim 2$. Likewise, for a range of angular resolution of $\theta_{1/2} \sim 1610 - 3860$ mas we pay a penalty in sensitivity of $\lesssim 1.5$.

This configuration has an pseudo-random position of the antennas. The features of the resulting taperability curve are similar to the ones from the ngVLA Mid-baseline subarray, i.e., the loss of sensitivity for increasingly large uv-tapers is steep.

Figure 19 shows examples of 1D East-West cuts through example PSFs. Due to the distribution of the antennas, the resulting PSFs are very Gaussian-like at all angular resolutions. Notice that natural weighting with a uv-taper produces a very similar PSF to using robust $R = -0.5$ and a somewhat larger uv-taper.

Table 13 in Appendix D shows the key performance metrics of the ngVLA Core subarray using 94 antennas, tabulated for a range of selected resolutions between 1000 and 100000 mas. These metrics include the change in sensitivity corresponding to the uv-taper needed to achieve these resolutions (based on Figure 18 and the frequency scaling described in Section 3).

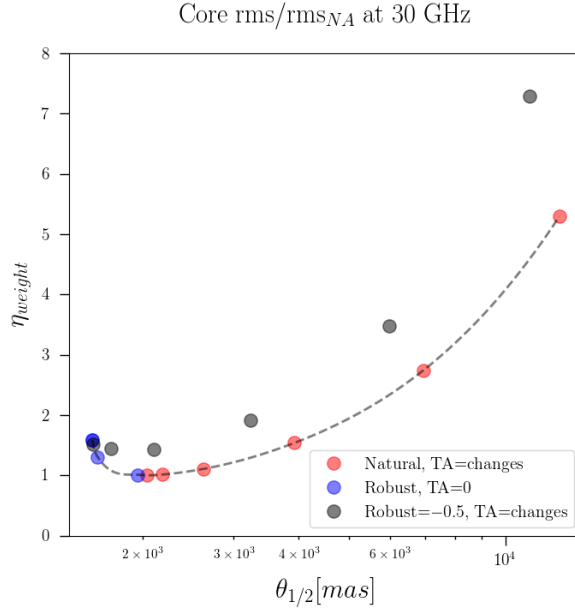


Figure 18: Taperability curve for the ngVLA Core subarray showing the image noise (rms) at different angular resolutions (FWHM) achieved by varying the imaging weights, simulated at 30 GHz. The noise has been scaled relative to that of the naturally weighted image (rms_{NA}). Symbols and colors are the same as used in Figure 3.

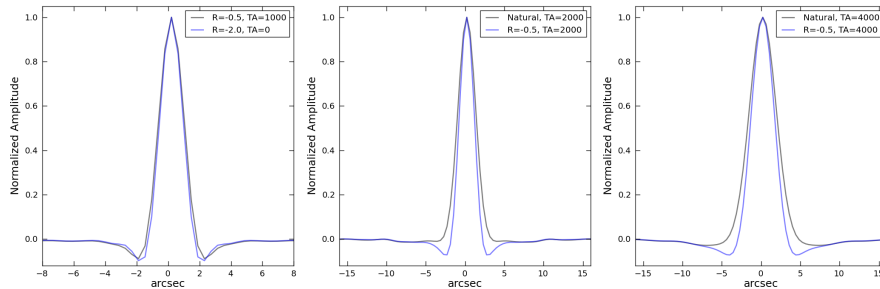


Figure 19: Simulated 30 GHz PSFs for the ngVLA Core subarray over a range of resolutions, showing the effect of different imaging weights (TA: uv-taper in mas, R: Briggs robust parameter). The PSFs are a selection of the data presented in Table 7. These examples illustrate how combinations of robustness and tapering allow for a beam of much higher quality (but at the expense of sensitivity).

4 Conclusions

I performed a set of simulations at 30 GHz for selected subarrays that are part of the current ngVLA reference design. I imaged each simulation with a range of uv-tapers to study the taperability of each subarray (i.e., the change in sensitivity versus resolution). I use these results to provide tables of key performance metrics (Appendix D) for each subarray at several representative resolutions. These results may also be incorporated into sensitivity calculations at arbitrary frequencies and resolutions by interpolating the data in the taperability figures.

The range of resolutions for each of the selected subarrays for which we pay a penalty in sensitivity of $\lesssim 2$ are:

- a. Main + LBA: $0.5 \leq \theta(\text{mas}) \leq 1000$
- b. LBA: $0.2 \leq \theta(\text{mas}) \leq 0.8$
- c. Main: $4 \leq \theta(\text{mas}) \leq 1000$
- d. Mid: $3 \leq \theta(\text{mas}) \leq 10$
- e. Plains+Core: $80 \leq \theta(\text{mas}) \leq 2700$
- f. Core: $1600 \leq \theta(\text{mas}) \leq 5200$

I also studied how the use of robust imaging weights affects the sensitivity and properties of the PSF over a range of resolutions for each subarray. The ngVLA Main+LBA, Main and Plains+Core subarrays produce a PSF with a broad skirt when using natural weighting, but this is reduced substantially by using Briggs weighting with a value of robust $R = -0.5$. The typical loss of sensitivity from using robust $R = -0.5$ instead of natural is less than a factor of two. The naturally weighted beams for the Mid-baseline and Core subarrays are quite Gaussian due to their more uniform distribution of baseline lengths, and therefore use of Briggs weighting with these subarrays is not advisable.

From our results, we conclude that the current ngVLA reference design has a high degree of taperability, i.e., that it can accommodate a wide range of resolutions without a great loss of sensitivity. For all of the subarrays that contain the dense core of antennas, the natural weighted beam is not Gaussian but we have presented weighting schemes that mitigate the PSF's broad skirt at the resolutions required by the KSGs. These weighting schemes, which decrease the sensitivity a factor $\lesssim 2$, represent a first approximation of the beam sculpting which may be required for certain high fidelity observations.

Appendix A Formulas

The following formulas were used to derive the values in the Key Performance tables 8, 9, 10, 11, 12 and 13.

Field of view The half-power beam width of an antenna assuming an uniform illumination pattern is:

$$\theta_{HPBW} \approx 1.02 \frac{\lambda}{D} [rad] \quad (1)$$

or a very rough estimate in more useful units is given by the following relation:

$$\theta_{HPBW} \approx 1.02 \frac{206265}{60} \frac{c}{\nu D} \approx \frac{1.05 \times 10^3}{\nu_{[GHz]} D_{[m]}} [arcmin] \quad (2)$$

Resolution of max. baseline (Synthesized Beam)

$$\theta_{max} \approx \frac{\lambda}{b_{max}} [rad] \approx \frac{6.2 \times 10^4}{\nu_{[GHz]} b_{max}[m]} [arcsec] \quad (3)$$

where b_{max} is the largest baseline (see Table 1) of the interferometer.

Total Effective Area The total collecting area is related to the antenna aperture efficiency η_A , the diameter of the antenna D and the total number of antennas N_{ant} :

$$A_{eff} = \eta_A N_{ant} A = \eta_A N_{ant} \pi \left(\frac{D}{2}\right)^2 [m^2] \quad (4)$$

System Equivalent Flux Density (SEFD) The system equivalent flux density of a single antenna is:

$$SEFD = 10^{26} \frac{2k_B T_{sys}}{\eta_Q \eta_A A} [Jy] \quad (5)$$

where k_B is the Boltzmann's constant, η_Q is the digitizer quantization efficiency (0.93), η_A is the antenna efficiency (see key performance metric tables), and A is the antenna's geometric collecting area in m^2 .

Naturally Weighted Point Source Sensitivity (σ_{NA}) The theoretical thermal noise or point-source rms expected for an image using natural weighting of the uv data is:

$$\sigma_{NA} = 10^6 \frac{SEFD}{\eta_c \sqrt{n_{pol} N_{ant} (N_{ant} - 1) t_{int} \Delta\nu}} [\mu Jy beam^{-1}] \quad (6)$$

where η_c is the correlator efficiency (0.98), n_{pol} is the number of polarizations (2), $\Delta\nu$ is the bandwidth in Hz, t_{int} is the integration time in seconds, and N_{ant} is the total number of antennas. Bandwidth used is either the ‘Max inst. bandwidth’ for continuum cases or the 10 km/s channel width for spectral line rms in the Key Performance tables.

Note that the RMS and the standard deviation are expected to be the same since the image mean is expected to be zero. Therefore, RMS and standard deviation are often used interchangeably except when specifically discussed in Section 3.1.

Weighted Point Source Sensitivity (σ_{rms})

$$\sigma_{rms} = \eta_{weight} \sigma_{NA} [\mu Jy beam^{-1}] \quad (7)$$

where the efficiency factor applied to the natural rms can be estimated using the blue and red data from Figures 3, 6, 9, 12, 15 and 18 and by scaling $\theta_{1/2}$ with frequency as $\theta_{1/2@30GHz} = \theta_{1/2@v} \times (\nu/30 \text{ GHz})$, where $\theta_{1/2}$ is in mas.

Line Width

$$\Delta\nu = \nu \frac{\Delta v}{c} \quad (8)$$

where the velocity resolution, Δv , and the speed of light in a vacuum, c , are both in m/s. The frequency ν is in Hz.

Brightness Temperature (σ_{TB})

$$\sigma_{TB} = 1.216 \frac{\sigma_{rms}}{\nu^2 \theta_{1/2}^2} [\text{K}] \quad (9)$$

where σ_{rms} is the point source sensitivity in $\mu Jy beam^{-1}$, $\theta_{1/2}$ is the resolution (FWHM) of the synthesized beam in arcseconds, and ν is the center frequency in GHz.

Appendix B Script of the Simulations

```
## To be run in CASA
import os

## configuration file
conf_file = 'ngvla-revC.cfg'

## Make an ASCII file with the configuration file i.e.,
change the extension from .cfg to .tab
tabname = 'antenna_positions_'+conf_file.split('.cfg')[0]+' .tab'
```

```

## The file above is called 'antenna_positions_ngvla-revB_lb.tab'

## Create a CASA table from an ASCII table using the table
utilities (tb) tool
tb.fromascii(tabname, conf_file, firstline=3, sep=' ',
columnnames=['X','Y','Z','DIAM','NAME'], datatypes=['D','D','D','D','A'])

xx=[]; yy=[]; zz=[];
xx = tb.getcol('X')           ## antenna positions
yy = tb.getcol('Y')
zz = tb.getcol('Z')
diam = tb.getcol('DIAM')      ## diameter of the antennas
anames = tb.getcol('NAME')    ## name of each antenna
tb.close()

## Setting the observation framework making our resource,
## similar to what we would do in the OPT when setting up our observations
## Simulate measurement set using the simulation utilities (sm) tool
ms_name = 'ngVLA_244_ant_1s.ms' ## Name of your measurement set

%os.system('rm -rf '+ ms_name)
sm.open( ms_name )

## Get the position of the ngVLA using the measures utilities (me)
pos_ngVLA = me.observatory('ngvla')

## set the antenna configuration using the sm tool using the positions,
## diameter and names of the antennas as read from the configuration file
sm.setconfig(telescopename = 'ngvla', x = xx, y = yy, z = zz,
             dishdiameter = diam, mount = 'alt-az',
             antname = list(anames), padname = list(anames),
             coordsystem = 'global', referencelocation = pos_ngVLA)

## set the spectral windows, in this case is a single channel
simulation with a channel resolution of 1 MHz and bandwidth of 1 MHz
sm.setspwindow(spwname = 'KBand', freq = '30GHz', deltafreq = '1MHz',
freqresolution = '1MHz', nchannels = 1, stokes = 'RR RL LR LL')

## set feed parameters for the antennas
sm.setfeed('perfect R L')

## set the field of observation that we are going to simulate
## (where the telescope is pointing), in this example we are using
## a Dec of +24deg
sm.setfield(sourcename='My source',
            sourcedirection=['J2000','00h0m0.0','+24.0.0.000'])

```

```

## set the limit of the observation for the antennas
sm.setlimits(shadowlimit=0.001, elevationlimit='8.0deg')

## weight to assign autocorrelation
sm.setauto(autocorrwt=0.0)

## integration time or how often the array writes one visibility
integrationtime = '1s'
sm.settimes(integrationtime = integrationtime, usehourangle = True,
            referencetime = me.epoch('utc', 'today'))

## setting the observation time, which for our example is 4 h
starttime = '-2h'
stoptime = '2h'
sm.observe('My source', 'KBand', starttime = starttime, stoptime = stoptime)

## Adding noise with 'simplenoise'

## set the noise level
sm.setnoise(mode='simplenoise', simplenoise='1Jy')

## adds the noise: calculate random Gaussian numbers and add to visibilities
sm.corrupt()

sm.close()

```

Appendix C Tables of the Simulation Parameters and Statistics

Table 2: Main + LBA Simulation Parameters and Statistics.

Robust	Taper	Cell	Beam	rms/rms _{NA}	σ/σ_{NA}
	[mas]	[mas]	[mas] × [mas]		
-2.0	0.0	0.05	0.649 × 0.212	2.733e+00	4.430e+00
-1.6	0.0	0.05	0.656 × 0.223	2.169e+00	3.517e+00
-1.2	0.0	0.05	0.688 × 0.248	1.698e+00	2.752e+00

Table 2 – Continued on next page

Table 2 – Continued from previous page

Robust	Taper	Cell	Beam	rms/rms _{NA}	σ/σ_{NA}
	[mas]	[mas]	[mas] × [mas]		
−0.8	0.0	0.05	0.759 × 0.278	1.295e+00	2.100e+00
−0.4	0.0	0.05	0.826 × 0.314	1.008e+00	1.634e+00
+0.0	0.0	0.05	0.899 × 0.380	8.617e-01	1.397e+00
+0.4	0.0	0.05	1.003 × 0.446	7.738e-01	1.251e+00
+0.8	0.0	0.05	1.128 × 0.517	7.286e-01	1.112e+00
Natural	0.0	0.05	1.395 × 0.659	1.000e+00	1.000e+00
Natural	0.5	0.0625	2.335 × 1.786	1.032e+00	1.136e+00
Natural	1.0	0.125	5.231 × 3.912	8.066e-01	1.279e+00
Natural	2.0	0.25	9.521 × 7.368	1.071e+00	1.311e+00
Natural	4.0	0.5	16.144 × 13.170	8.412e-01	1.357e+00
Natural	8.0	1.0	33.955 × 24.341	8.235e-01	1.335e+00
Natural	16.0	2.0	63.056 × 49.858	8.265e-01	1.337e+00
Natural	32.0	4.0	116.161 × 102.381	8.628e-01	1.398e+00
Natural	64.0	8.0	180.617 × 174.704	8.909e-01	1.444e+00
Natural	128.0	16.0	307.371 × 304.017	9.630e-01	1.561e+00
Natural	256.0	32.0	596.361 × 591.457	1.082e+00	1.755e+00
Natural	512.0	64.0	1094.505 × 1089.448	1.218e+00	1.974e+00
Natural	1024.0	128.0	1770.341 × 1738.472	1.382e+00	2.241e+00
Natural	2048.0	256.0	2563.633 × 2521.097	1.660e+00	2.691e+00
−0.5	0.0	0.05	0.881 × 0.367	8.902e-01	1.443e+00
−0.5	0.5	0.0625	1.320 × 1.008	9.595e-01	1.555e+00
−0.5	1.0	0.125	3.178 × 2.388	9.442e-01	1.531e+00
−0.5	2.0	0.25	5.684 × 4.371	9.719e-01	1.576e+00
−0.5	4.0	0.5	8.932 × 7.315	1.022e+00	1.657e+00
−0.5	8.0	1.0	17.593 × 12.418	1.099e+00	1.781e+00
−0.5	16.0	2.0	30.395 × 23.620	1.182e+00	1.916e+00
−0.5	32.0	4.0	57.384 × 48.695	1.265e+00	2.050e+00
−0.5	64.0	8.0	93.468 × 88.899	1.318e+00	2.137e+00
−0.5	128.0	16.0	150.198 × 144.066	1.389e+00	2.252e+00

Table 2 – Continued on next page

Table 2 – Continued from previous page

Robust	Taper	Cell	Beam	rms/rms _{NA}	σ/σ_{NA}
	[mas]	[mas]	[mas]×[mas]		
-0.5	256.0	32.0	297.254 × 285.075	1.579e+00	2.560e+00
-0.5	512.0	64.0	622.363 × 605.247	1.702e+00	2.759e+00
-0.5	1024.0	128.0	1224.905 × 1209.979	1.802e+00	2.921e+00
-0.5	2048.0	256.0	2004.015 × 1989.253	2.009e+00	3.257e+00

Table 3: LBA Simulation Parameters and Statistics.

Robust	Taper	Cell	Beam	rms/rms _{NA}	σ/σ_{NA}
	[mas]	[mas]	[mas]×[mas]		
-2.0	0.0	0.058	0.420 × 0.128	1.860e+00	1.860e+00
+0.0	0.0	0.058	0.421 × 0.134	1.335e+00	1.335e+00
+1.0	0.0	0.058	0.444 × 0.171	1.011e+00	1.011e+00
Natural	0.0	0.058	0.458 × 0.180	1.000e+00	1.000e+00
Natural	0.5	0.058	0.748 × 0.476	1.593e+00	1.593e+00
Natural	1.0	0.058	1.354 × 1.218	2.622e+00	2.622e+00
Natural	2.0	0.058	4.226 × 3.224	3.727e+00	3.727e+00
Natural	4.0	0.058	8.983 × 5.809	4.295e+00	4.295e+00
-0.5	0.0	0.058	0.420 × 0.129	1.684e+00	1.684e+00
-0.5	0.5	0.058	0.619 × 0.316	2.270e+00	2.270e+00
-0.5	1.0	0.058	0.978 × 0.846	4.033e+00	4.033e+00
-0.5	2.0	0.058	2.536 × 1.927	6.799e+00	6.799e+00
-0.5	4.0	0.058	7.630 × 3.767	8.454e+00	8.454e+00

Table 4: Main array Spiral 214 Simulation Parameters and Statistics.

Robust	Taper	Cell	Beam	rms/rms _{NA}	σ/σ_{NA}
	[mas]	[mas]	[mas]×[mas]		
-2.0	0.0	0.52	3.447 × 2.348	2.967e+00	2.969e+00
-1.0	0.0	0.52	4.359 × 3.281	1.728e+00	1.729e+00

Table 4 – Continued on next page

Table 4 – Continued from previous page

Robust	Taper	Cell	Beam	rms/rms _{NA}	σ/σ_{NA}
	[mas]	[mas]	[mas]×[mas]		
+0.0	0.0	0.52	6.851 × 5.583	1.168e+00	1.169e+00
Natural	0.0	0.52	9.327 × 7.679	1.000e+00	1.000e+00
Natural	1.0	0.52	9.762 × 8.087	1.002e+00	1.002e+00
Natural	2.0	0.52	11.077 × 9.274	1.014e+00	1.014e+00
Natural	4.0	0.52	16.302 × 13.274	1.056e+00	1.056e+00
Natural	8.0	0.52	31.236 × 22.446	1.118e+00	1.117e+00
Natural	16.0	0.52	57.807 × 44.599	1.188e+00	1.188e+00
Natural	32.0	0.52	107.139 × 91.144	1.263e+00	1.263e+00
Natural	64.0	0.52	169.546 × 162.566	1.341e+00	1.341e+00
Natural	128.0	0.52	278.393 × 273.537	1.487e+00	1.486e+00
Natural	256.0	0.52	537.257 × 531.862	1.711e+00	1.709e+00
Natural	512.0	0.52	1003.030 × 999.264	1.985e+00	1.982e+00
Natural	1024.0	0.52	1700.064 × 1669.093	2.336e+00	2.331e+00
Natural	2048.0	0.52	2506.229 × 2482.328	2.895e+00	2.886e+00
−0.5	0.0	0.52	5.469 × 4.398	1.373e+00	1.374e+00
−0.5	1.0	0.52	5.690 × 4.630	1.363e+00	1.364e+00
−0.5	2.0	0.52	6.370 × 5.291	1.361e+00	1.362e+00
−0.5	4.0	0.52	9.104 × 7.429	1.430e+00	1.431e+00
−0.5	8.0	0.52	16.649 × 11.958	1.558e+00	1.559e+00
−0.5	16.0	0.52	29.028 × 22.384	1.709e+00	1.710e+00
−0.5	32.0	0.52	52.678 × 44.047	1.878e+00	1.879e+00
−0.5	64.0	0.52	85.553 × 81.930	1.940e+00	1.941e+00
−0.5	128.0	0.52	131.621 × 128.793	1.963e+00	1.964e+00
−0.5	256.0	0.52	238.973 × 237.061	2.071e+00	2.073e+00
−0.5	512.0	0.52	458.987 × 457.988	2.121e+00	2.123e+00
−0.5	1024.0	0.52	905.928 × 905.928	2.145e+00	2.146e+00
−0.5	2048.0	0.52	1800.706 × 1798.934	2.357e+00	2.352e+00

Table 5: Mid-baseline Simulation Parameters and Statistics.

Robust	Taper	Cell	Beam	rms/rms _{NA}	σ/σ_{NA}
	[mas]	[mas]	[mas] × [mas]		
-2.0	0.0	0.52	3.052 × 2.107	1.437e+00	1.437e+00
+0.0	0.0	0.52	3.109 × 2.174	1.286e+00	1.286e+00
+1.0	0.0	0.52	3.817 × 2.774	1.012e+00	1.012e+00
Natural	0.0	0.52	4.096 × 2.971	1.000e+00	1.000e+00
Natural	1.0	0.52	4.250 × 3.138	1.003e+00	1.003e+00
Natural	2.0	0.52	4.714 × 3.673	1.032e+00	1.032e+00
Natural	4.0	0.52	6.430 × 5.156	1.197e+00	1.197e+00
Natural	8.0	0.52	10.579 × 8.435	1.585e+00	1.585e+00
Natural	16.0	0.52	17.079 × 14.887	2.372e+00	2.372e+00
Natural	32.0	0.52	31.843 × 28.577	4.143e+00	4.143e+00
-0.5	0.0	0.52	3.058 × 2.116	1.413e+00	1.413e+00
-0.5	1.0	0.52	3.143 × 2.239	1.374e+00	1.374e+00
-0.5	2.0	0.52	3.415 × 2.591	1.328e+00	1.328e+00
-0.5	4.0	0.52	4.664 × 3.733	1.441e+00	1.441e+00
-0.5	8.0	0.52	8.314 × 6.584	1.952e+00	1.952e+00
-0.5	16.0	0.52	3.922 × 11.921	2.901e+00	2.901e+00
-0.5	32.0	0.52	24.902 × 23.449	5.161e+00	5.161e+00

Table 6: Plains+Core Simulation Parameters and Statistics.

Robust	Taper	Cell	Beam	rms/rms _{NA}	σ/σ_{NA}
	[mas]	[mas]	[mas] × [mas]		
-2.0	0.0	14	79.519 × 71.913	2.194e+00	2.194e+00
-1.0	0.0	14	80.572 × 72.838	1.992e+00	1.992e+00
+0.0	0.0	14	100.689 × 93.815	1.332e+00	1.332e+00
+1.0	0.0	14	151.854 × 145.835	1.022e+00	1.022e+00
Natural	0.0	14	166.184 × 159.968	1.000e+00	1.000e+00
Natural	32.0	14	175.810 × 169.818	1.003e+00	1.003e+00
Natural	64.0	14	203.182 × 197.905	1.024e+00	1.024e+00

Table 6 – Continued on next page

Table 6 – Continued from previous page

Robust	Taper	Cell	Beam	rms/rms _{NA}	σ/σ_{NA}
	[mas]	[mas]	[mas]×[mas]		
Natural	128.0	14	300.550 × 297.122	1.112e+00	1.112e+00
Natural	256.0	14	548.831 × 543.879	1.252e+00	1.252e+00
Natural	512.0	14	1009.496 × 1006.698	1.412e+00	1.412e+00
Natural	1024.0	14	1688.602 × 1663.915	1.602e+00	1.602e+00
Natural	2048.0	14	2538.076 × 2497.251	1.915e+00	1.915e+00
Natural	4096.0	14	4009.201 × 3975.590	2.743e+00	2.743e+00
-0.5	0.0	14	85.271 × 77.725	1.634e+00	1.634e+00
-0.5	32.0	14	89.419 × 81.936	1.582e+00	1.582e+00
-0.5	64.0	14	101.528 × 94.340	1.516e+00	1.516e+00
-0.5	128.0	14	146.987 × 141.268	1.584e+00	1.584e+00
-0.5	256.0	14	266.358 × 257.780	1.863e+00	1.863e+00
-0.5	512.0	14	499.290 × 488.865	2.121e+00	2.121e+00
-0.5	1024.0	14	944.452 × 936.097	2.091e+00	2.091e+00
-0.5	2048.0	14	1821.350 × 1819.384	1.845e+00	1.845e+00
-0.5	4096.0	14	3595.607 × 3595.468	3.071e+00	3.071e+00

Table 7: Core Simulation Parameters and Statistics.

Robust	Taper	Cell	Beam	rms/rms _{NA}	σ/σ_{NA}
	[mas]	[mas]	[mas]×[mas]		
-2.0	0.0	420	1627.166 × 1580.187	1.587e+00	1.587e+00
-1.0	0.0	420	1627.593 × 1580.822	1.579e+00	1.579e+00
+0.0	0.0	420	1659.987 × 1621.662	1.306e+00	1.306e+00
+1.0	0.0	420	1988.750 × 1923.023	1.009e+00	1.009e+00
Natural	0.0	420	2081.468 × 2002.126	1.000e+00	1.000e+00
Natural	1000.0	420	2220.016 × 2161.020	1.012e+00	1.012e+00
Natural	2000.0	420	2648.026 × 2595.526	1.105e+00	1.105e+00
Natural	4000.0	420	3944.700 × 3912.348	1.538e+00	1.538e+00
Natural	8000.0	420	6981.323 × 6923.797	2.741e+00	2.741e+00
Natural	16000.0	420	12803.217 × 12588.734	5.293e+00	5.292e+00

Table 7 – Continued on next page

Table 7 – Continued from previous page

Robust	Taper	Cell	Beam	rms/rms _{NA}	σ/σ_{NA}
	[mas]	[mas]	[mas] × [mas]		
-0.5	0.0	420	1631.297 × 1586.166	1.519e+00	1.519e+00
-0.5	1000.0	420	1756.164 × 1725.343	1.441e+00	1.441e+00
-0.5	2000.0	420	2105.822 × 2101.485	1.433e+00	1.433e+00
-0.5	4000.0	420	3254.244 × 3208.549	1.920e+00	1.920e+00
-0.5	8000.0	420	6014.961 × 5915.736	3.477e+00	3.477e+00
-0.5	16000.0	420	11229.789 × 11028.851	7.295e+00	7.291e+00

Appendix D Key Performance Metrics

Table 8: Next Generation VLA Key Performance Metrics

Parameters [units]	2.4 GHz	8 GHz	16 GHz	27 GHz	41 GHz	93 GHz	Notes
Band Lower Frequency, f_L [GHz]	1.2	3.5	12.3	20.5	30.5	70.0	a
Band Upper Frequency, f_U [GHz]	3.5	12.3	20.5	34.0	50.5	116.0	a
Field of view [arcmin]	24.3	7.3	3.6	2.2	1.4	0.6	b
Aperture efficiency [%]	0.77	0.76	0.87	0.85	0.81	0.58	b
Total effective area, A_{eff} [10^3 m ²]	47.8	47.1	53.8	52.6	50.4	36.0	b
System temperature, T_{sys} [K]	25	27	28	35	56	103	a,f
Max. inst. bandwidth [GHz]	2.3	8.8	8.2	13.5	20.0	20.0	a
Antenna SEFD [Jy]	372.3	419.1	372.1	485.1	809.0	2080.5	a, b
Resolution of max. baseline (θ_{max}) [mas]	2.91	0.87	0.44	0.26	0.17	0.07	c
Natural Resolution							
Continuum rms, 1 hr [μ Jy/beam]	0.38	0.22	0.20	0.21	0.28	0.73	d
Line width, 10 km/s [kHz]	80.1	266.9	533.7	900.6	1367.6	3102.1	
Line rms, 1 hr, 10 km/s [μ Jy/beam]	65.0	40.1	25.2	25.2	34.2	58.3	d

Table 8 – Continued on next page

Table 8 – Continued from previous page

1000 mas Resolution ($\theta_{1/2}$)							
Continuum rms, 1 hr, Robust [μ Jy/beam]	0.52	0.34	0.35	0.39	0.59	2.24	e
Line rms, 1 hr, 10 km/s, Robust [μ Jy/beam]	88.9	61.1	43.3	47.9	70.9	179.6	e
TB rms continuum, 1 hr, Robust [K]	0.1107	0.0064	0.0017	0.0007	0.0004	0.0003	e
TB rms line, 1 hr, 10 km/s, Robust [K]	18.76	1.16	0.21	0.08	0.05	0.03	e
100 mas Resolution ($\theta_{1/2}$)							
Continuum rms, 1 hr, Robust [μ Jy/beam]	0.50	0.30	0.27	0.28	0.40	1.14	e
Line rms, 1 hr, 10 km/s, Robust [μ Jy/beam]	85.0	53.6	33.6	34.8	48.4	91.3	e
TB rms continuum, 1 hr, Robust [K]	10.58	0.56	0.13	0.05	0.03	0.02	e
TB rms line, 1 hr, 10 km/s, Robust [K]	1794.1	101.9	15.9	5.8	3.5	1.3	e
10 mas Resolution ($\theta_{1/2}$)							
Continuum rms, 1 hr, Robust [μ Jy/beam]	0.41	0.27	0.26	0.27	0.38	0.97	e
Line rms, 1 hr, 10 km/s, Robust [μ Jy/beam]	69.9	48.3	32.4	33.2	46.3	77.7	e
TB rms continuum, 1 hr, Robust [K]	870.58	50.51	12.42	4.53	2.77	1.36	e
TB rms line, 1 hr, 10 km/s, Robust [K]	1E5	9173	1540	555	335	109	e
1 mas Resolution ($\theta_{1/2}$)							
Continuum rms, 1 hr, Robust [μ Jy/beam]	-	20.87	0.31	0.21	0.29	0.90	e
Line rms, 1 hr, 10 km/s, Robust [μ Jy/beam]	-	3789.8	38.2	25.7	34.7	72.0	e
TB rms continuum, 1 hr, Robust [K]	-	4E5	1466	350	207	126	e
TB rms line, 1 hr, 10 km/s, Robust [K]	-	7E7	2E5	42813	25073	10119	e

Table 8 – Continued on next page

Table 8 – Continued from previous page

0.1 mas Resolution ($\theta_{1/2}$)							
Continuum rms, 1 hr, Robust [μ Jy/beam]	-	-	-	-	-	20.96	e
Line rms, 1 hr, 10 km/s, Robust [μ Jy/beam]	-	-	-	-	-	1683.2	e
TB rms continuum, 1 hr, Robust [K]	-	-	-	-	-	3E5	e
TB rms line, 1 hr, 10 km/s, Robust [K]	-	-	-	-	-	2E7	e

a – 6-band 'baseline' receiver configuration.

b – Reference design concept of 244 18m aperture antennas. Unblocked aperture with 160 μ m surface.

c – Current reference design configuration. Resolution in EW axis.

d – Point source sensitivity using natural imaging weights, dual polarization and all baselines (Main array + LBA).

e – Using Weights as described in the text, scaled by frequency.

f – Average over band. Assumes 1 mm PWV at 93 GHz, 6 mm PWV for other bands, 45 deg elevation on sky.

For the latest performance estimates please visit the ngVLA website:

ngvla.nrao.edu/page/refdesign

Table 9: Next Generation VLA LBA Subarray Key Performance Metrics

Parameters [units]	2.4 GHz	8 GHz	16 GHz	27 GHz	41 GHz	93 GHz	Notes
Band Lower Frequency, f_L [GHz]	1.2	3.5	12.3	20.5	30.5	70.0	a
Band Upper Frequency, f_U [GHz]	3.5	12.3	20.5	34.0	50.5	116.0	a
Field of view [arcmin]	24.3	7.3	3.6	2.2	1.4	0.6	b
Aperture efficiency [%]	0.77	0.76	0.87	0.85	0.81	0.58	b
Total effective area, A_{eff} [10^3 m ²]	5.9	5.8	6.6	6.5	6.2	4.4	b
System temperature, T_{sys} [K]	25	27	28	35	56	103	a,f
Max. inst. bandwidth [GHz]	2.3	8.8	8.2	13.5	20.0	20.0	a
Antenna SEFD [Jy]	372.3	419.1	372.1	485.1	809.0	2080.5	a, b
Resolution of max. baseline (θ_{max}) [mas]	2.91	0.87	0.44	0.26	0.17	0.07	c
Natural Resolution							
Continuum rms, 1 hr [μ Jy/beam]	3.17	1.82	1.68	1.70	2.33	6.00	d
Line width, 10 km/s [kHz]	80.1	266.9	533.7	900.6	1367.6	3102.1	
Line rms, 1 hr, 10 km/s [μ Jy/beam]	536.5	330.8	207.6	208.4	282.1	481.6	d
10 mas Resolution ($\theta_{1/2}$)							
Continuum rms, 1 hr, Robust [μ Jy/beam]	6.35	6.24	6.80	7.56	10.96	30.30	e
Line rms, 1 hr, 10 km/s, Robust [μ Jy/beam]	1075.7	1132.8	842.3	926.0	1324.9	2433.2	e
TB rms continuum, 1 hr, Robust [K]	13397.57	1185.17	322.77	126.16	79.25	42.60	e
TB rms line, 1 hr, 10 km/s, Robust [K]	2E6	2E5	40007.99	15446.73	9584.26	3420.91	e

Table 9 – Continued on next page

Table 9 – Continued from previous page

1 mas Resolution ($\theta_{1/2}$)							
Continuum rms, 1 hr, Robust [μ Jy/beam]	-	1.85	2.43	3.68	6.27	21.43	e
Line rms, 1 hr, 10 km/s, Robust [μ Jy/beam]	-	335.39	300.61	450.57	757.86	1720.87	e
TB rms continuum, 1 hr, Robust [K]	-	35091.11	11519.75	6138.61	4533.36	3013.24	e
TB rms line, 1 hr, 10 km/s, Robust [K]	-	6E6	1E6	7.5E5	5E5	2E5	e
0.1 mas Resolution ($\theta_{1/2}$)							
Continuum rms, 1 hr, Robust [μ Jy/beam]	-	-	-	-	-	6.15	e
Line rms, 1 hr, 10 km/s, Robust [μ Jy/beam]	-	-	-	-	-	493.75	e
TB rms continuum, 1 hr, Robust [K]	-	-	-	-	-	86455.92	e
TB rms line, 1 hr, 10 km/s, Robust [K]	-	-	-	-	-	7E6	e

a – 6-band 'baseline' receiver configuration.

b – Reference design concept of 30 18m aperture antennas. Unblocked aperture with 160 μ m surface.

c – Current reference design configuration. Resolution in EW axis.

d – Point source sensitivity using natural imaging weights, dual polarization.

e – Using Weights as described in the text, scaled by frequency.

f – Average over band. Assumes 1 mm PWV at 93 GHz, 6 mm PWV for other bands, 45 deg elevation on sky.

For the latest performance estimates please visit the ngVLA website:

ngvla.nrao.edu/page/refdesign

Table 10: Next Generation VLA Main Subarray Key Performance Metrics

Parameters [units]	2.4 GHz	8 GHz	16 GHz	27 GHz	41 GHz	93 GHz	Notes
Band Lower Frequency, f_L [GHz]	1.2	3.5	12.3	20.5	30.5	70.0	a
Band Upper Frequency, f_U [GHz]	3.5	12.3	20.5	34.0	50.5	116.0	a
Field of view [arcmin]	24.3	7.3	3.6	2.2	1.4	0.6	b
Aperture efficiency [%]	0.77	0.76	0.87	0.85	0.81	0.58	b
Total effective area, A_{eff} [10^3 m ²]	41.9	41.3	47.2	46.1	44.2	31.5	b
System temperature, T_{sys} [K]	25	27	28	35	56	103	a,f
Max. inst. bandwidth [GHz]	2.3	8.8	8.2	13.5	20.0	20.0	a
Antenna SEFD [Jy]	372.3	419.1	372.1	485.1	809.0	2080.5	a, b
Resolution of max. baseline (θ_{max}) [mas]	25.64	7.69	3.85	2.28	1.50	0.66	c
Natural Resolution							
Continuum rms, 1 hr [μ Jy/beam]	0.44	0.25	0.23	0.24	0.32	0.83	d
Line width, 10 km/s [kHz]	80.1	266.9	533.7	900.6	1367.6	3102.1	
Line rms, 1 hr, 10 km/s [μ Jy/beam]	74.1	45.7	28.7	28.8	39.0	66.5	d
1000 mas Resolution ($\theta_{1/2}$)							
Continuum rms, 1 hr, Robust [μ Jy/beam]	0.54	0.37	0.40	0.45	0.70	2.80	e
Line rms, 1 hr, 10 km/s, Robust [μ Jy/beam]	91.8	67.4	49.0	55.6	84.1	224.8	e
TB rms continuum, 1 hr, Robust [K]	0.1144	0.0071	0.0019	0.0008	0.0005	0.0004	e
TB rms line, 1 hr, 10 km/s, Robust [K]	19.38	1.28	0.23	0.09	0.06	0.03	e

Table 10 – Continued on next page

Table 10 – Continued from previous page

100 mas Resolution ($\theta_{1/2}$)							
Continuum rms, 1 hr, Robust [μ Jy/beam]	0.44	0.28	0.28	0.29	0.42	1.26	e
Line rms, 1 hr, 10 km/s, Robust [μ Jy/beam]	73.89	51.08	34.24	36.06	50.85	101.33	e
TB rms continuum, 1 hr, Robust [K]	9.20	0.53	0.13	0.05	0.03	0.02	e
TB rms line, 1 hr, 10 km/s, Robust [K]	1559.81	97.05	16.26	6.01	3.68	1.42	e
10 mas Resolution ($\theta_{1/2}$)							
Continuum rms, 1 hr, Robust [μ Jy/beam]	-	0.86	0.29	0.24	0.34	0.94	e
Line rms, 1 hr, 10 km/s, Robust [μ Jy/beam]	-	156.70	36.40	28.87	40.84	75.43	e
TB rms continuum, 1 hr, Robust [K]	-	163.95	13.95	3.93	2.44	1.32	e
TB rms line, 1 hr, 10 km/s, Robust [K]	-	29773.06	1728.82	481.50	295.40	106.05	e

a – 6-band 'baseline' receiver configuration.

b – Reference design concept of 214 18m aperture antennas. Unblocked aperture with 160 μ m surface.

c – Current reference design configuration. Resolution in EW axis.

d – Point source sensitivity using natural imaging weights, dual polarization.

e – Using Weights as described in the text, scaled by frequency.

f – Average over band. Assumes 1 mm PWV at 93 GHz, 6 mm PWV for other bands, 45 deg elevation on sky.

For the latest performance estimates please visit the ngVLA website:

ngvla.nrao.edu/page/refdesign

Table 11: Next Generation VLA Mid-baseline Subarray Key Perform. Metrics

Parameters [units]	2.4 GHz	8 GHz	16 GHz	27 GHz	41 GHz	93 GHz	Notes
Band Lower Frequency, f_L [GHz]	1.2	3.5	12.3	20.5	30.5	70.0	a
Band Upper Frequency, f_U [GHz]	3.5	12.3	20.5	34.0	50.5	116.0	a
Field of view [arcmin]	24.3	7.3	3.6	2.2	1.4	0.6	b
Aperture efficiency [%]	0.77	0.76	0.87	0.85	0.81	0.58	b
Total effective area, A_{eff} [10^3 m ²]	9.0	8.9	10.1	9.9	9.5	6.8	b
System temperature, T_{sys} [K]	25	27	28	35	56	103	a,f
Max. inst. bandwidth [GHz]	2.3	8.8	8.2	13.5	20.0	20.0	a
Antenna SEFD [Jy]	372.3	419.1	372.1	485.1	809.0	2080.5	a, b
Resolution of max. baseline (θ_{max}) [mas]	25.64	7.69	3.85	2.28	1.50	0.66	c
Natural Resolution							
Continuum rms, 1 hr [μ Jy/beam]	2.05	1.18	1.09	1.10	1.51	3.89	d
Line width, 10 km/s [kHz]	80.1	266.9	533.7	900.6	1367.6	3102.1	
Line rms, 1 hr, 10 km/s [μ Jy/beam]	347.8	214.4	134.6	135.1	182.9	312.2	d
100 mas Resolution ($\theta_{1/2}$)							
Continuum rms, 1 hr, Robust [μ Jy/beam]	2.91	4.39	7.31	11.22	20.83	91.20	e
Line rms, 1 hr, 10 km/s, Robust [μ Jy/beam]	494.0	797.1	906.1	1373.8	2518.4	7322.9	e
TB rms continuum, 1 hr, Robust [K]	61.5	8.3	3.5	1.9	1.5	1.3	e
TB rms line, 1 hr, 10 km/s, Robust [K]	10427.9	1514.6	430.4	229.1	182.2	102.9	e

Table 11 – Continued on next page

Table 11 – Continued from previous page

10 mas Resolution ($\theta_{1/2}$)							
Continuum rms, 1 hr, Robust [μ Jy/beam]	-	1.43	1.25	1.69	3.16	16.50	e
Line rms, 1 hr, 10 km/s, Robust [μ Jy/beam]	-	259.4	155.0	206.9	382.17	1324.5	e
TB rms continuum, 1 hr, Robust [K]	-	271.4	59.4	28.2	22.9	23.2	e
TB rms line, 1 hr, 10 km/s, Robust [K]	-	49295.8	7363.9	3450.5	2764.5	1862.2	e
1 mas Resolution ($\theta_{1/2}$)							
Continuum rms, 1 hr, Robust [μ Jy/beam]	-	-	-	-	-	3.9	e
Line rms, 1 hr, 10 km/s, Robust [μ Jy/beam]	-	-	-	-	-	312.4	e
TB rms continuum, 1 hr, Robust [K]	-	-	-	-	-	547.0	e
TB rms line, 1 hr, 10 km/s, Robust [K]	-	-	-	-	-	43921.5	e

a – 6-band 'baseline' receiver configuration.

b – Reference design concept of 46 18m aperture antennas. Unblocked aperture with 160 μ m surface.

c – Current reference design configuration. Resolution in EW axis.

d – Point source sensitivity using natural imaging weights, dual polarization.

e – Using Weights as described in the text, scaled by frequency.

f – Average over band. Assumes 1 mm PWV at 93 GHz, 6 mm PWV for other bands, 45 deg elevation on sky.

For the latest performance estimates please visit the ngVLA website:

ngvla.nrao.edu/page/refdesign

Table 12: Next Generation VLA Plains+Core Subarray Key Perform. Metrics

Parameters [units]	2.4 GHz	8 GHz	16 GHz	27 GHz	41 GHz	93 GHz	Notes
Band Lower Frequency, f_L [GHz]	1.2	3.5	12.3	20.5	30.5	70.0	a
Band Upper Frequency, f_U [GHz]	3.5	12.3	20.5	34.0	50.5	116.0	a
Field of view [arcmin]	24.3	7.3	3.6	2.2	1.4	0.6	b
Aperture efficiency [%]	0.77	0.76	0.87	0.85	0.81	0.58	b
Total effective area, A_{eff} [10^3 m ²]	32.9	32.4	37.1	36.2	34.7	24.8	b
System temperature, T_{sys} [K]	25	27	28	35	56	103	a,f
Max. inst. bandwidth [GHz]	2.3	8.8	8.2	13.5	20.0	20.0	a
Antenna SEFD [Jy]	372.3	419.1	372.1	485.1	809.0	2080.5	a, b
Resolution of max. baseline (θ_{max}) [mas]	715.70	214.71	107.36	63.62	41.90	18.47	c
Natural Resolution							
Continuum rms, 1 hr [μ Jy/beam]	0.56	0.32	0.29	0.30	0.41	1.06	d
Line width, 10 km/s [kHz]	80.1	266.9	533.7	900.6	1367.6	3102.1	
Line rms, 1 hr, 10 km/s [μ Jy/beam]	94.5	58.2	36.6	36.7	49.7	84.8	d
10000 mas Resolution ($\theta_{1/2}$)							
Continuum rms, 1 hr, Robust [μ Jy/beam]	0.75	0.64	1.07	1.86	3.85	20.18	e
Line rms, 1 hr, 10 km/s, Robust [μ Jy/beam]	127.3	115.6	133.0	228.1	465.2	1620.78	e
TB rms continuum, 1 hr, Robust [K]	0.001590	0.00012	0.00005	0.00003	0.00003	0.00003	e
TB rms line, 1 hr, 10 km/s, Robust [K]	0.26880	0.0220	0.0063	0.0038	0.0034	0.0023	e

Table 12 – Continued on next page

Table 12 – Continued from previous page

1000 mas Resolution ($\theta_{1/2}$)							
Continuum rms, 1 hr, Robust [μ Jy/beam]	0.84	0.35	0.37	0.41	0.62	2.33	e
Line rms, 1 hr, 10 km/s, Robust [μ Jy/beam]	141.92	63.20	45.57	50.63	75.10	187.43	e
TB rms continuum, 1 hr, Robust [K]	0.1768	0.0066	0.0018	0.0007	0.0004	0.0003	e
TB rms line, 1 hr, 10 km/s, Robust [K]	29.96	1.20	0.22	0.08	0.05	0.03	e
100 mas Resolution ($\theta_{1/2}$)							
Continuum rms, 1 hr, Robust [μ Jy/beam]	-	-	-	0.36	0.46	1.18	e
Line rms, 1 hr, 10 km/s, Robust [μ Jy/beam]	-	-	-	43.66	55.26	95.04	e
TB rms continuum, 1 hr, Robust [K]	-	-	-	0.06	0.03	0.02	e
TB rms line, 1 hr, 10 km/s, Robust [K]	-	-	-	7.28	4.00	1.34	e

a – 6-band 'baseline' receiver configuration.

b – Reference design concept of 168 18m aperture antennas. Unblocked aperture with 160 μ m surface.

c – Current reference design configuration. Resolution in EW axis.

d – Point source sensitivity using natural imaging weights, dual polarization.

e – Using Weights as described in the text, scaled by frequency.

f – Average over band. Assumes 1 mm PWV at 93 GHz, 6 mm PWV for other bands, 45 deg elevation on sky.

For the latest performance estimates please visit the ngVLA website:

ngvla.nrao.edu/page/refdesign

Table 13: Next Generation VLA Core Subarray Key Performance Metrics

Parameters [units]	2.4 GHz	8 GHz	16 GHz	27 GHz	41 GHz	93 GHz	Notes
Band Lower Frequency, f_L [GHz]	1.2	3.5	12.3	20.5	30.5	70.0	a
Band Upper Frequency, f_U [GHz]	3.5	12.3	20.5	34.0	50.5	116.0	a
Field of view [arcmin]	24.3	7.3	3.6	2.2	1.4	0.6	b
Aperture efficiency [%]	0.77	0.76	0.87	0.85	0.81	0.58	b
Total effective area, A_{eff} [10^3 m ²]	18.4	18.1	20.7	20.3	19.4	13.8	b
System temperature, T_{sys} [K]	25	27	28	35	56	103	a,f
Max. inst. bandwidth [GHz]	2.3	8.8	8.2	13.5	20.0	20.0	a
Antenna SEFD [Jy]	372.3	419.1	372.1	485.1	809.0	2080.5	a, b
Resolution of max. baseline (θ_{max}) [mas]	20612.2	6183.7	3091.8	1832.2	1206.6	531.9	c
Natural Resolution							
Continuum rms, 1 hr [μ Jy/beam]	1.00	0.57	0.53	0.54	0.74	1.89	d
Line width, 10 km/s [kHz]	80.1	266.9	533.7	900.6	1367.6	3102.1	
Line rms, 1 hr, 10 km/s [μ Jy/beam]	169.2	104.3	65.5	65.7	89.0	151.9	d
100000 mas Resolution ($\theta_{1/2}$)							
Continuum rms, 1 hr, Robust [μ Jy/beam]	3.21	5.64	7.69	9.65	14.96	44.05	e
Line rms, 1 hr, 10 km/s, Robust [μ Jy/beam]	544.0	1023.4	953.7	1181.8	1809.5	3536.9	e
TB rms continuum, 1 hr, Robust [K]	0.00007	0.00001	4E-6	2E-6	1E-6	6E-7	e
TB rms line, 1 hr, 10 km/s, Robust [K]	0.01148	0.00194	0.00045	0.00020	0.00013	0.00005	e

Table 13 – Continued on next page

Table 13 – Continued from previous page

10000 mas Resolution ($\theta_{1/2}$)							
Continuum rms, 1 hr, Robust [μ Jy/beam]	-	0.64	1.09	1.97	4.18	20.48	e
Line rms, 1 hr, 10 km/s, Robust [μ Jy/beam]	-	116.57	135.11	241.47	505.98	1644.72	e
TB rms continuum, 1 hr, Robust [K]	-	0.00012	0.00005	0.00003	0.00003	0.00003	e
TB rms line, 1 hr, 10 km/s, Robust [K]	-	0.02215	0.00642	0.00403	0.0037	0.00231	e
1000 mas Resolution ($\theta_{1/2}$)							
Continuum rms, 1 hr, Robust [μ Jy/beam]	-	-	-	-	-	2.36	e
Line rms, 1 hr, 10 km/s, Robust [μ Jy/beam]	-	-	-	-	-	189.76	e
TB rms continuum, 1 hr, Robust [K]	-	-	-	-	-	0.00033	e
TB rms line, 1 hr, 10 km/s, Robust [K]	-	-	-	-	-	0.027	e

a – 6-band 'baseline' receiver configuration.

b – Reference design concept of 94 18m aperture antennas. Unblocked aperture with 160 μ m surface.

c – Current reference design configuration. Resolution in EW axis.

d – Point source sensitivity using natural imaging weights, dual polarization.

e – Using Weights as described in the text, scaled by frequency.

f – Average over band. Assumes 1 mm PWV at 93 GHz, 6 mm PWV for other bands, 45 deg elevation on sky.

For the latest performance estimates please visit the ngVLA website:

ngvla.nrao.edu/page/refdesign

References

- [1] Alberto Bolatto, Shami Chatterjee, et. al., *Next Generation Very Large Array Memo No. 19 Key Science Goals For The Next Generation Very Large Array (Ngvla): Report From The Ngvla Science Advisory Council*.
- [2] Chris Carilli, *Next Generation Very Large Array Memo No. 12 The Strength of the Core*.

- [3] Chris Carilli, Y. Shao, *Next Generation Very Large Array Memo No. 13 Imaging Capabilities: High Redshift CO.*
- [4] Chris Carilli, *Next Generation Very Large Array Memo No. 16 More on Synthesized Beams and Sensitivity.*
- [5] Chris Carilli, Alan Erickson, *Next Generation VLA Memo. 41 Initial Imaging Tests of the Spiral Configuration.*
- [6] Chris Carilli, *Next Generation Very Large Array Memo No. 47 Resolution and Sensitivity of ngvla-revB.*
- [7] Barry Clark, Walter Brisken, *Next Generation Very Large Array Memo No. 3 Possible Configurations for the ngVLA.*
- [8] Eric Murphy, Rob Selina, ngVLA SAC, *ngVLA Science Requirements document 020.10.15.00.00-0001-REQ.*
- [9] Luca Ricci, et. al., *Next Generation Very Large Array Memo No. 33 Investigating The Early Evolution Of Planetary Systems With Alma And The Next Generation Very Large Array.*

The National Radio Astronomy Observatory and Green Bank Observatory are facilities of the U.S. National Science Foundation operated under cooperative agreement by Associated Universities, Inc. This work was supported by awards AST-2034328 (MSIP Prototype Antenna) and AST-2334267 (ngVLA Design Activities); NRAO related activities are funded under award AST-1647378 (NRAO Operations/Development).

